

## INITIAL OPERATION OF THE FIRST 20 MEV TANK OF THE INR LINAC

Yu. V. Bylinsky, A. N. Drugakov, S. K. Esin, Yu. K. Fatkulin, A. P. Fedotov, A. V. Feschenko, S. G. Garylkapov, D. V. Gorelov, Yu. V. Kiselev, A. N. Mirzojan, B. P. Murin, P. N. Ostroumov, I. A. Sagin, V. L. Serov  
Institute for Nuclear Research, Academy of Sciences of USSR  
Moscow 117312 USSR

### Introduction

The  $H^+$ ,  $H^-$  linac of the INR meson facility is under tuning now. The results on the cavities tuning were reported in EPAC-88 [1]. Recently the initial operation of the first 20 MeV Alvarez tank have been completed. The beam acceleration have been provided at 1 Hz repetition rate but the tank have been driven at 10 Hz.

80 mA 750 keV proton beam was successfully transported to the tank entrance. To set the rf amplitude and phase the small (5 ÷ 10 mA) and high (up to 80 mA) pulse current of the injected beam have been used.

The tank 1 tuning includes the following procedures:

- determination and steering of the beam position at the tank entrance;
- emittance measurement in the low energy beam channel and transverse beam matching;
- preliminary investigation of the 6-dimensional matching by using rf-buncher and focusing elements;
- determination of the nominal rf amplitude;
- determination of the nominal injection energy and the high voltage divider calibration;
- determination of the phase and amplitude of two-cavity buncher;
- production of the 50 mA design pulse current, measurements of the transverse and longitudinal parameters.

The beam dynamic simulation has been used for the linac tuning [2,3]. By using multiparticle model a variety of the beam parameters including the influence of the electric and geometric errors on the beam behaviour have been studied in the 6-dimensional phase space. The sketch of main experimental equipment is shown in the Fig.1.

### 1. Determination of the injection energy and rf amplitude

The determination of the rf amplitude is closely connected with the injection energy determination that is well looked from the calculated curves (Fig.2). The experimental procedure of the rf amplitude and injection energy determination is the following (the buncher is off):

- rough determination of the rf amplitude (with the precision of 4%) at the injection energy also known with error of 2%;
- precise determination of the injection energy by using the phase difference of the field excited by accelerated beam in the third harmonic resonant detectors;
- precise determination of the rf amplitude taking into account precisely known injection energy;
- the using of the Bunch Length Monitor (BLM) for the measurement of the rf amplitude with the precision of about 0.2%. This measurement has a rather weak dependance of the injection energy;
- more precise determination of the rf amplitude and the injection energy by the comparison of the results obtained from the amplitude scan and from the phase spectrum measure-

ments.

Let's consider each stage of the experiment. To determine the injection energy we use the dependence of the bunch coherent displacement at the tank exit as a function of the injection energy taking rf amplitude as a parameter. For that it is sufficiently to know roughly the absolute value of the accelerating field. The experimental dependence of the phase difference between the two-3-rd harmonic monitors, spaced in a distance  $L$ , vs accelerating field level are presented in Fig.3. It is clear that the amplitude of the coherent phase oscillation depends essentially upon the injection energy. That allows to determine the injection energy. At the known injection energy the nominal rf amplitude is found from the data shown in Fig.2. For the first cavity of the INR linac  $E_0 = E_c / 0.835$  where  $E_c$  corresponds to the rf field at which the bucket disappears. By comparison the theoretical and experimental data it is possible to determine the injection energy with the accuracy of a few keV.

The typical dependence of the accelerated beam current measured beyond the copper foil of 0.46 mm thickness vs rf amplitude is shown in Fig.4.

For more precise determination of the  $E_c$  the extrapolation of the experimental curve is used. The experimental curves in Fig.4 for the various injection energies are in a good agreement with the theoretical data in Fig.2.

A new possibility for precise determination of the rf amplitude have been opened with BLM development and test [4]. This device is perfectly adequate for the rf amplitude determination due to very high sensitivity of the bunch shape vs accelerating field. The maximum value of the phase spectrum is achieved for the total phase advance of  $\Psi = 3.75\pi$  at the exit of the tank which corresponds to accelerating field  $E' = 0.995E_0$ . Because the phase advance does not depend on the injection energy the nominal rf amplitude can be determined for any injection energy. In turn as soon as the rf amplitude is precisely determined the injection energy can be easily found by using the method described above.

To decrease the various errors influence on the accuracy of the phase spectrum the measurements have been conducted using automatic phase and amplitude control. The measurements have shown that for the injection current of 10 mA the rf amplitude and phase errors are not more than  $\pm 0.25\%$  and  $\pm 0.5^\circ$  respectively. The intrapulse ripple of the injection energy was equal  $\pm 0.25\%$  and have been caused by the pulse top oscillation of the 750 kV transformer. The injection energy instability from pulse to pulse was an order of magnitude better. The typical measured phase spectra are presented in Fig.5. The nominal accelerating field according to the maximum of  $I_m$  is found by approximation of the data. Similar measurements have been done for the injection energy  $0.99W_0$ . It turns out that the accuracy of the  $E'$  determination is about

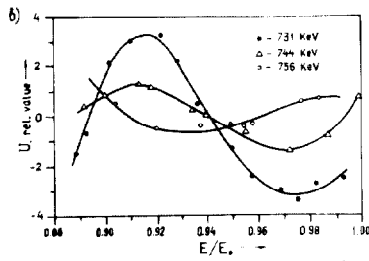


Fig. 3  
Experimental signal proportional to phase difference of the excited field in the harmonic monitors vs the rf amplitude at the various injection energies.

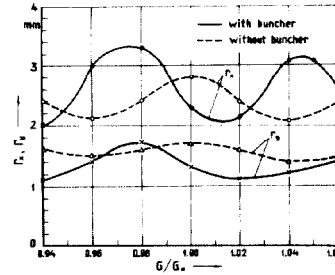


Fig. 8  
Rms  $r_x, r_y$  without (---) and with (—) buncher vs focusing gradient  $G/G_0$ .

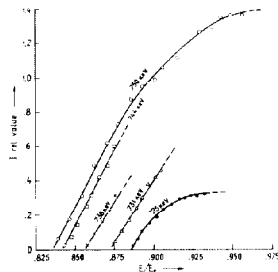


Fig. 4  
Experimental dependence of accelerated beam current on the rf amplitude at the various injection energies.

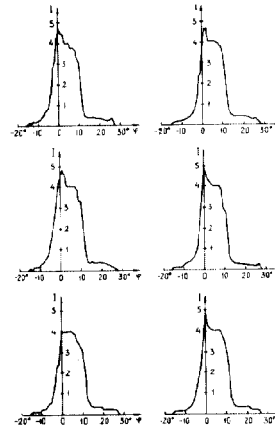


Fig. 9  
Phase spectra of the accelerated beam.

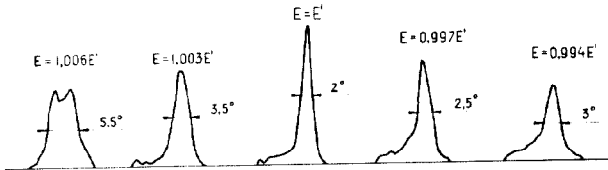


Fig. 5  
Experimental phase spectra of the accelerated beam for the various rf amplitude.

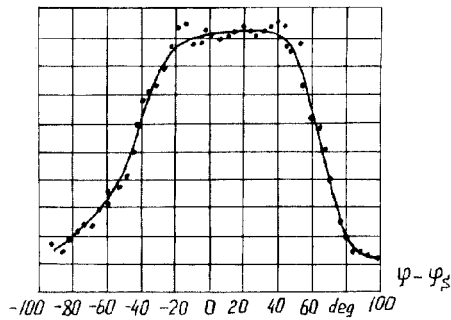


Fig. 6  
Phase scan results for the buncher at the nominal rf amplitudes.

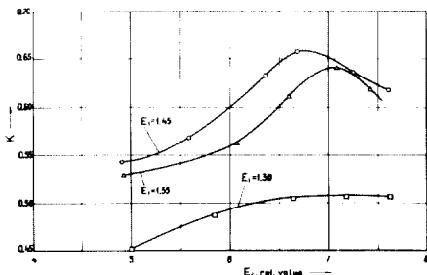


Fig. 7  
Experimental acceleration efficiency vs rf amplitudes in bunching cavities.

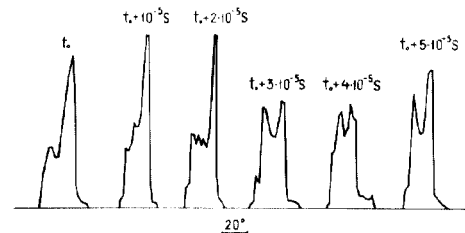


Fig. 10  
Phase spectra sampling for various time delay.

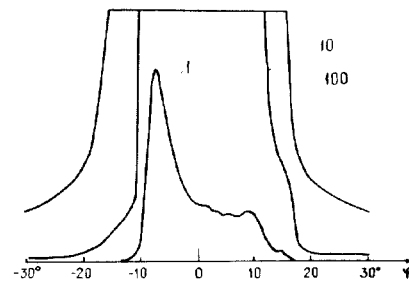


Fig. 11  
Phase spectra for the various BLM gain.

0.1%. An analysis of the experimental data and the accuracy of the rf amplitude determination according to the maximum  $I_m$  allows to conclude that the rf amplitude error is less than 0.2%.

## 2. The two-cavity buncher amplitude and phase setting

There is two-cavity buncher at the entrance of the first tank. The setting of rf phase in the cavities is carried out by using of the phase scan while the first tank is excited to the nominal field level. Because the phase scan results depend on the beam intensity the phase setting runs are conducted at the relatively small current of  $5 \pm 10$  mA. The typical experimental curve of the phase scan is presented in Fig.6.

Next the dependence of the accelerated current from the rf amplitude in bunching cavities  $I=f(E_1, E_2)$  is taken. The values of  $E_1$  and  $E_2$  are set according to the maximum value of accelerating efficiency (Fig.7).

## 3. The beam parameters measurement

The beam transverse parameters are studied using two profile monitors, mounted spaced in a distance of 0.6 m. After the installation of the second linac tank the intratank distance will be 19 cm which allows the only single profile monitor to be introduced. Therefore we investigate the possibility to obtain the maximum information from a single profile monitor. It is known, that by using the profile monitor one may find the coherent oscillation amplitude and determine the beam mismatch with the periodically focusing channel [5]. These data are used for the beam steering at the tank entrance. More detail study of these data allows to obtain rms values of the phase ellipse by measuring the beam size for the various strengths of the focusing channel (there are 44 focusing periods in INR tank 1). For this purpose the dependence of the rms beam sizes  $r_x$  and  $r_y$  as a function of focusing gradient  $G/G_0$  in all quadrupole lenses have been taken. The typical behaviour of  $r_{x,y}$  is shown in Fig.8. By using data of  $r_{xm}, r_{ym}, r_{x0}$  (Fig.8) rms emittance and rms parameters  $\alpha, \beta, \gamma$  are calculated.

By knowing rms parameters it is possible to match the beam at the tank entrance more carefully. For example  $r_x, r_y$  behaviour is shown in Fig.8 for two mode of tank 1 operation: with and without buncher operation.

The measurement of longitudinal beam parameters was carried out by using BLM. To get the phase spectrum of the bunch the secondary emission current from BLM wire target vs the

phase of the 594.6 MHz (3-rd harmonic of the accelerating frequency) deflecting field was measured. The signal was whether integrated along the beam macropulse (Fig.9) or sampled at a given 5 mks interval of that pulse (Fig.10). The phase shift and decrement of the phase oscillations in the first tank are rather big. It makes the longitudinal phase portrait to be close to the canonical ellipse. In such a case the momentum spread  $\Delta P/P$  and bunch length  $\Phi$  are connected as

$$\frac{\Delta P}{P} \cdot \frac{\Delta P}{P} = \frac{\Omega \cdot \gamma^2}{\omega}$$

where  $\omega$ —accelerating frequency,  $\Omega$ —phase oscillation frequency. Having the full measured width of the bunch  $20^\circ-30^\circ$  (100% of particles) we can derive momentum spread  $\Delta P/P = \pm(1.0-1.5)\%$ .

At the exit of the tank 1 unaccelerated particles are presented. BLM measurements outside of the bunch length show that the fraction of unaccelerated particles at the exit of tank 1 is less than 1%. Making BLM sensitivity increased it turns to be possible to study longitudinal halo of the beam. The phase spectra measured with various amplification are presented in Fig.11. The flat top of the curves corresponds to the saturation. The adjustment of the amplification is carried out by changing of the photomultiplier voltage. The preliminary calibration of BLM was done using thermoelectrons [4].

Authors are greatly indebted to operators of various accelerator systems for their help required for these experiments.

## References

1. Yu. V. Bylinsky et al. "Meson Factory Accelerating Structure Tuning", EPAC, Rome, June 7-11, 1988.
2. R. A. Jameson et al. "Longitudinal Tuning of the LAMPF 201.25 MHz Linac Without Space Charge", Los Alamos Scientific Laboratory report LA-6863, 1978.
3. V. A. Batalin et al. "Beam Transportation Through the 100 MeV Proton Linac", Preprint HEPI, ING 69-9, Serpuchov, 1969.
4. A. V. Feschenko, P. N. Ostroumov. "Bunch Shape Measuring Technique and its Application for an Ion Linac Tuning", 1986 Linac Conference, Stanford, June 2-6, 1986.
5. A. Browman and J. Hurd, Los Alamos Scientific Laboratory, Private Communication, 1988.

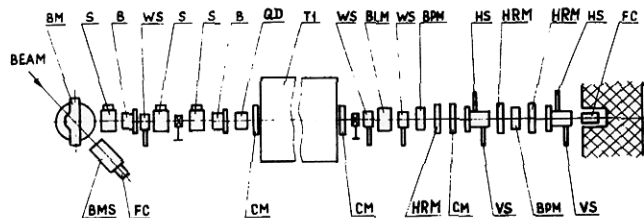


Fig.1

The layout of the experimental equipment. Legend: BM—bending magnet, BMS—emittance monitor FC—Faraday cup, S—solenoid, B—buncher, WS—wire scanner, QD—quadrupole doublet, T1—tank 1, CM—current monitor, BLM—bunch length monitor, BPM—bunch position monitor, HRM—harmonic resonant monitor, VS—vertical slit, HS—horizontal slit.

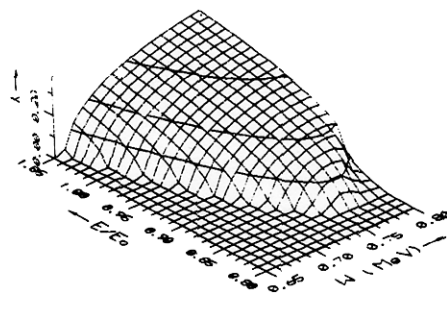


Fig.2

The theoretical dependence of accelerating efficiency for monochromatic beam on rf amplitude and injection energy.